9th ANKARA INTERNATIONAL AEROSPACE CONFERENCE **AIAC-2017-134**
20-22 September 2017 - METU, Ankara TURKEY

VEHICLE WIND NOISE PREDICTION THROUGH SOLUTIONS OF NAVIER-STOKES AND FFOWCS WILLIAMS & HAWKINGS

Baran GÜMÜŞ[1] and Ezgi GÜNEŞ[2]
Ford Otosan
İstanbul, Turkey

Yusuf ÖZYÖRÜK
Middle East Technical University
Ankara, Turkey

ABSTRACT

The aim of this study is to calculate flow noise of a car model at a far-field location. Aeroacoustic calculations for non-reduced models require excessive computing source. Ffowcs Williams – Hawkings (FW-H) method is one of the most effective methods of Computational Aero Acoustics (CAA) in terms of computational cost. The FW-H method is a hybrid method, which consists of a near field flow solution and then a linear acoustic propagation to far-field. Acoustic sources around the vehicle must be captured accurately. A detailed, unsteady turbulent flow simulation is required due to the nature of noise generation mechanisms. The sound generated by such sources is propagated to far-field using FW-H integral equations that are implemented in a FORTRAN code. The results are compared with a wind tunnel test.

INTRODUCTION

Vehicles are getting more and more quiet by the virtue of recent technological improvements. Since wind noise is one of the major contributors of total vehicle noise [Hucho, 2013], it must be limited to design quieter vehicles. Considering that wind tunnel tests are expensive, computational tools are effective in terms of required cost. There are many CAA applications using simplified box shaped car models in the literature [Fink, 1977; Yamamoto, Donelson et al., 1995; Bergamini, Casella et al., 1997; Sovani and Chen, 2005; Farassat and Casper, 2006; Kotapati, Keating et al., 2009; Hartmann, Ocker et al., 2012; Shorter, Blanchet et al., 2012; Blanchet, Golota et al., 2014; Blanchet, 2014]. This study consists of a non-reduced, non-simplified full vehicle model to simulate a real car shape noise.

Wind noise is related to turbulent, three dimensional, transient flow [Yalçın, 2015]. Accurate CAA methods are investigated and discussed in this study. Sound pressure levels are calculated at far-field, which is four meters away from vehicle. Currently, clay models are used for far-field aeroacoustics evaluations in basic design phases of development in automotive [Fuchs, Nijman et al., 2015].

A widely used hybrid CAA method is used in this study, the porous FW-H method. [Lyrintzis, 2003; Singer, Lockard et al., 2003; Lockard and Casper, 2005; Farassat and Casper, 2006;

[1] Product Development Engineer at Ford Otosan, Email: bgumus@ford.com.tr
[2] Product Development Engineer at Ford Otosan, Email: egunes3@ford.com.tr
[3] Professor in Aerospace Engineering Department, Email: yusuf.ozyoruk@ae.metu.edu.tr

Uosukainen, 2011; Yao, Davidson et al., 2012; Khan, 2014; Yalçın, 2015] uses FW-H method. This hybrid method consists of two parts, unsteady flow solution and linear acoustic propagation.

CFD simulation is the first step of an acoustic prediction. For this reason, flow solution must be calculated with high certainty. An accurate CFD simulation require mesh size limitation, an appropriate boundary layer modelling and suitable turbulence modelling for transient and steady analyses. The dimensionless wall distance y+, pressure and drag coefficients, residuals, Q-criterion are investigated to check the CFD analyses. Mesh dependence of the study is also checked. For convergence check, pressure distribution around vehicle side mirror is compared between steady results and mean values of transient time-steps. Residuals are normalized to double check convergence.

Then, acoustic propagation is done by an integration code, which is written in FORTRAN. In the end, calculated sound pressure levels are compared to a wind tunnel test with same conditions of Computational Fluid Dynamics (CFD) simulation.

The extent of this study is predicting sound waves up to 2.5 kHz. Currently, a fairly well correlation between test and prediction is obtained. Increasing the correlation level and maximum frequency are two main future works to adapt the study into real applications.

METHOD

The FW-H method is an extension of Lighthill's method [Lockard and Casper, 2005]. The method enforces all acoustic sources to be contained in a control surface. The surface is called as FW-H surface. Linear propagation is used by integrating FW-H equation from the FW-H surface to the far-field. In the original version, FW-H surface is not porous and require a volume integral. However, porous FW-H method does not require volume integration; if the surface is large enough to capture all turbulence. Acoustic sources inside the control surface should be solved with high accuracy

Porous Ffowcs Williams – Hawkings Method Details

The method can be applied both in time and frequency domain. In this study, frequency approach is used for its practicality. The N-S equation in form of wave equation is;

$$\left(\frac{\partial^2}{\partial t^2} - c_o^2 \frac{\partial^2}{\partial x_i \partial x_i}\right)(H(f)\rho') = \underbrace{\frac{\partial^2}{\partial x_i \partial x_i}\left(T_{ij}H(f)\right)}_{\text{Quadrupole}} \underbrace{- \frac{\partial}{\partial x_i}\left(F_i \delta(f)\right)}_{\text{Dipole}} \underbrace{+ \frac{\partial}{\partial t}\left(Q\delta(f)\right)}_{\text{Monopole}} \quad (1)$$

where,

$$T_{ij} = \rho u_i u_j + P_{ij} - c_0^2 \rho' \delta_{ij} \quad (2)$$

$$F_i = (P_{ij} + \rho u_i (u_j - v_j)) \frac{\partial f}{\partial x_j} \quad (3)$$

$$Q = (p_0 v_i + \rho(u_i - v_i)) \frac{\partial f}{\partial x_i} \quad (4)$$

Here, t represents time and x_i stands for Cartesian coordinates, with indices over three dimensions. Lighthill's stress tensor is denoted by T_{ij}, unsteady forces are represented by F_i and Q is the unsteady mass term. These terms stand for the quadrupole, dipole and monopole

terms respectively. Moreover, total density and total pressure are represented by ρ and p, respectively. The function f shows the domain outside the control surface. Normalization is applied by $|\nabla f| = 1$. The fluid velocities are denoted as u_i. The terms v_i are the velocities on f surface. The speed of sound at freestream is c_0. All free stream conditions are represented by subscript 0. Prime notation is means perturbation terms. The Kronecker delta is $\delta_{ij} = 1\ for\ i = j$ and it is zero if $i \neq j$. Similarly, Heaviside function is defined as; $H(f) = 1\ for\ f > 0\ and\ H(f) = 0\ for\ f < 0$. Finally, Dirac delta function $\delta(f)$ is derivative of the Heaviside function. $\delta(f) = 0\ for\ f \neq 0$ but integral of Dirac delta function from a region that includes f=0 leads to a finite value.

The frequency domain solution of the 3D FW-H equation is rewritten by [Lockard and Casper, 2005] as follows;

$$H(f)c_0^2\rho'(y,\omega) = I_T + I_L + I_Q \tag{5}$$

where, the monopole term;

$$I_T = -\int_{f=0} i\omega Q(\xi,\omega)G(y;\xi)ds \tag{6}$$

and the dipole term;

$$I_L = -\int_{f=0} F_i(\xi,\omega)\frac{\partial G(y;\xi)}{\partial y_i}ds \tag{7}$$

and the volumetric quadrupole term;

$$I_Q = -\int_{f>0} T_{ij}(\xi,\omega)\frac{\partial^2 G(y;\xi)}{\partial \xi_i \partial \xi_j}d\xi \tag{8}$$

Heaviside function on the left hand side of Equation 1 indicates zero solution on any point of FW-H surface. In [Lockard, 2000], T_{ij}, F_i and Q terms of quadrupole, dipole and monopole are simplified as follows;

$$T_{ij} = \rho u_i u_j + p\delta_{ij} - c_0^2\rho'\delta_{ij} \tag{9}$$

$$F_i = \left(p\delta_{ij} + \rho(u_i - 2U_i)u_j + \rho_0 U_i U_j\right)\hat{n}_j \tag{10}$$

$$Q = (\rho u_i - \rho_0 U_i)\hat{n}_i \tag{11}$$

The quadrupole term cannot be reduced. A typical approach for porous FW-H method is neglecting the quadrupole term by locating the FW-H surface outside the non-linear region, in which T_{ij} is powerful. Then, it is logical to ignore the quadrupole term.

For a flow in y1 direction, corresponding 3-D Green's function is as follows [Lockard and Casper, 2005];

$$G(x,y;\xi,\eta) = \frac{-1}{4\pi d}\exp\left(-ik\left(d - M\left(y_1 - \xi_1\right)\right)/\beta^2\right) \tag{12}$$

with complex number $i = \sqrt{-1}$. Prandtl-Glauert factor is $\beta = \sqrt{1 - M^2}$. Mach number is defined as $M = |U_i|/c_0$. The wavenumber term is $k = \omega/c_0$.
Also, d represents distances between sources and receiver;

$$d = \sqrt{(y_1 - \xi_1)^2 + \beta^2(y_2 - \xi_2)^2 + \beta^2(y_3 - \xi_3)^2} \tag{13}$$

Application of the Method

The main noise contributor parts of a car are shown simply in the Figure 1. Side mirror and A-pillar regions are the most effective regions [Zhengqi, Yiping et al., 2009]. Since the most effective region is around the A-pillar and side mirror, FW-H surface is located around this region and should be large enough to contain all turbulence of mirror and A-pillar as stated by [Lockard and Casper, 2005]. The surface consists of a porous region at outer part and viscous wall around vehicle geometry.

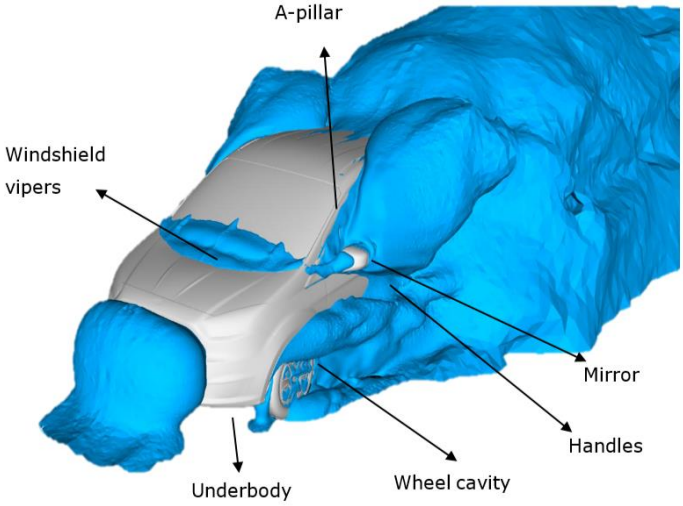

Figure 1: Main noise contributor parts of a car

The FW-H method requires history of flow variables, such as; pressure, velocities and density. Considering the fact that inflow velocity is around M=0.1, flow is assumed as incompressible. Then, unsteady pressure and velocity data of every cell of control surface are saved. Since the FW-H equation is in frequency domain, time history of cells is converted to frequency domain using Fast Fourier Transformation. However, complex flows are never periodic. First, a window function should be applied to make the history periodic. Many window functions are available in the literature. The most common window for this kind of application is Hanning window. An example is shown in Figure 2.

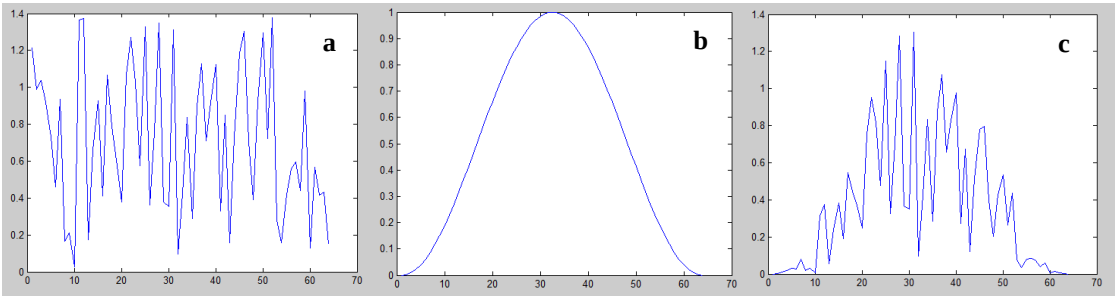

Figure 2: a-Random data, b- Hanning window, c- Windowed data

Wind Tunnel Testing

The wind tunnel test is conducted in Ford Merkenich wind tunnel. The placement of vehicle and microphone is shown in the Figure 3. The acoustic results are gathered 3 times and averages of these 3 runs are saved.

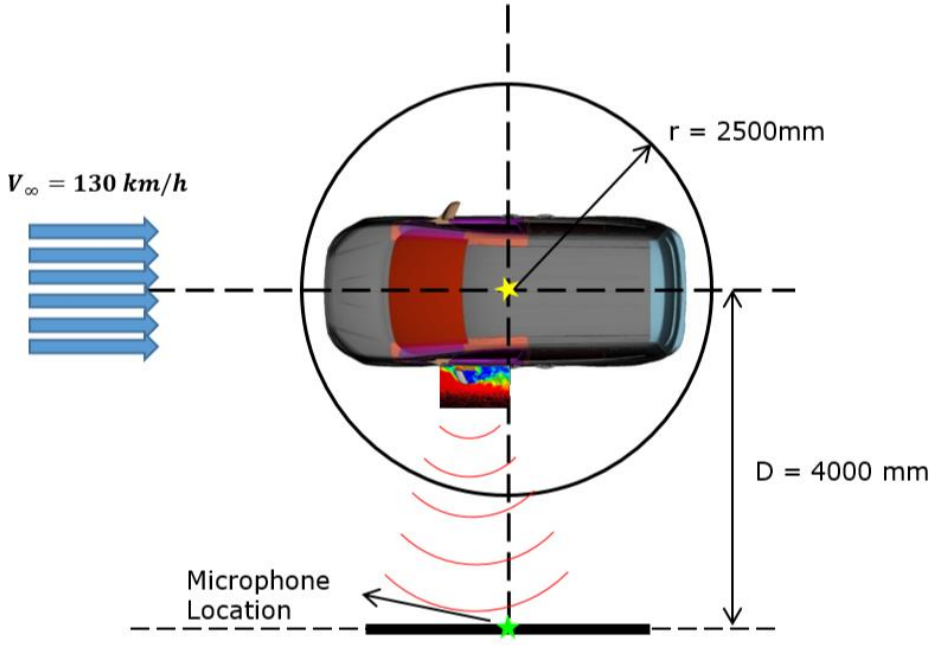

Figure 3: Wind tunnel test

Modelling the Vehicle

For simplification, the model is a half model, center plane is defined as symmetry plane, as in Figure 4. Total number of cells is around 60million.

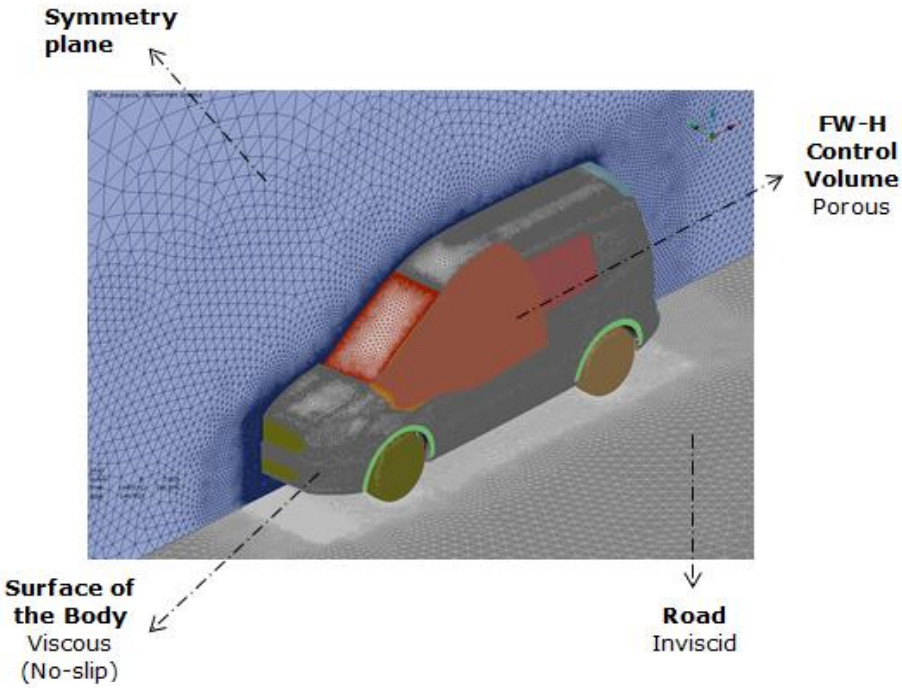

Figure 4: Representation of the half vehicle model

In order to obtain low y^+ values, i.e. less than 1 and wall function is not used. Near wall region is resolved all the way down to wall. The first boundary layer height is 0.01mm with 10 layers forming a total height of 2mm. The y+ distribution at given conditions is shown in Figure 5;

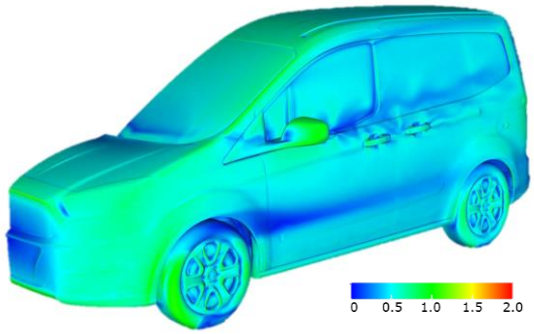

Figure 5: y+ Distribution on the vehicle model

A mesh dependence study is also conducted. Mesh around main noise sources is both improved and coarsened by 30%. Drag coefficient change is plotted in Figure 6 and visuals of mesh dependence test are shown in Figure 7.

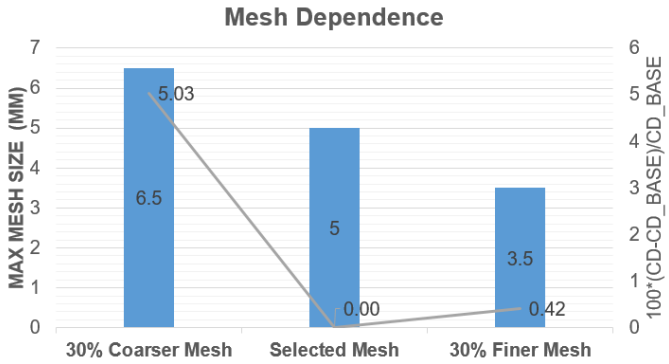

Figure 6: Mesh dependence for a 30% improvement/coarsening

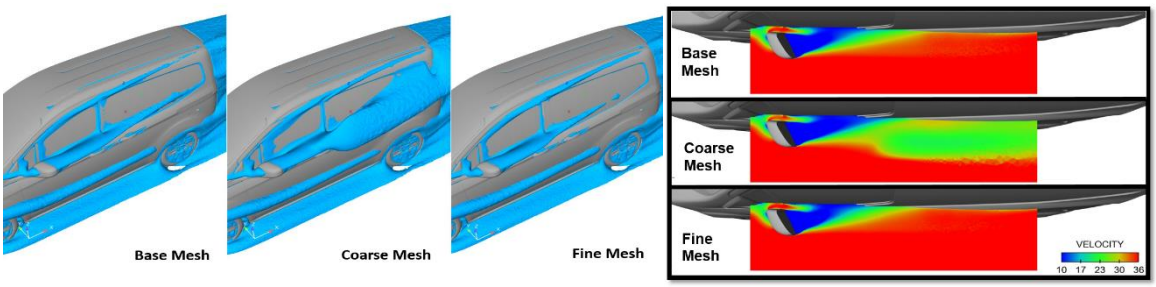

Figure 7: Mesh dependence visuals;

Left: Equal velocity bubbles, Right: Velocity distribution around side mirror

As seen from the mesh dependence study, although coarser meshes are very sensitive to flow solution, the finer meshes are that much effective. In other words, it can be stated that base mesh of base mesh (5mm, max) around mirror is fine enough to resolve flow domain.

CFD Simulation

Third order MUSCL scheme with combination of second order discretization is used. Before beginning iterations, geometric properties of FW-H surface are exported. For ease in convergence of transient analysis, the simulation begins with a steady state analysis that consists of 20k iterations. After reaching steady state, transient analysis starts.

The unsteady simulation has a 0.00002s time step with a total duration of 0.5 seconds. However, in order to "wait" for the vortex shedding mechanism to settle, first 0.1s is not saved. The relation between Strouhal number and Reynolds number in Equation 14 leads to a 0.033s settling time for vortex shedding of a real size vehicle side mirror. Assuming three periods are enough to have a settled vortex shedding, 0.1s is sufficient enough. After this point, flow properties are saved as history of each cell of FW-H surface.

$$f = St * V/D \tag{15}$$

Convergence of transient analysis is checked through residuals and pressure history around mirror. Residuals are normalized by the first value of unsteady analysis; therefore, residuals start from 1 and decrease by 1-2 orders, as seen from Figure 8. This is a good sign of unsteady convergence.

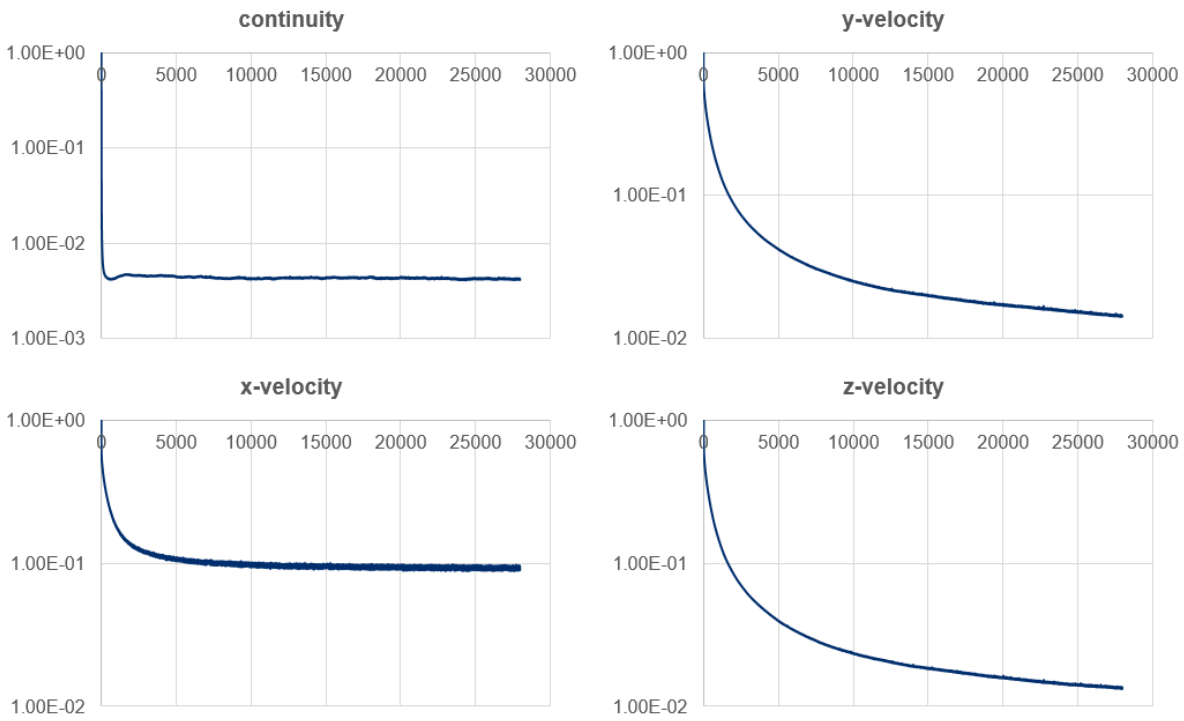

Figure 8: Normalized residual checks

Similarly, transient flow convergence is tested by 180 points on mirror. Steady state pressures are compared with average pressures of transient solution time-steps. The Figure 9 shows a good coherence.

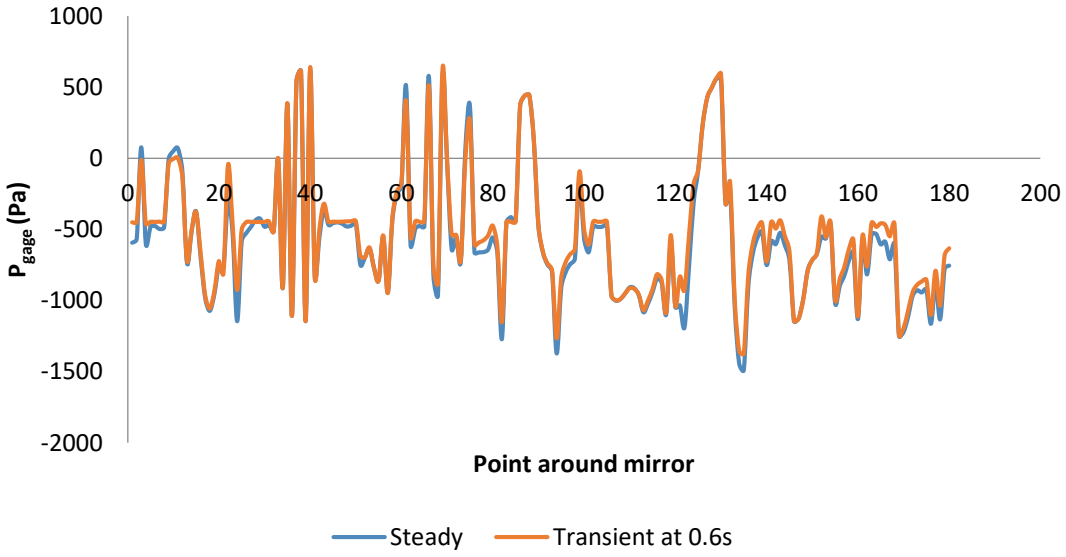

Figure 9: Transient flow convergence check

3D Ffowcs Williams – Hawkins Integral Code

The far-field propagation is done by an integration code written in FORTRAN. Pressure and velocity histories are combined with normal vectors and locations of cell centers of FW-H surface cells. All these data together form far-field noise levels.

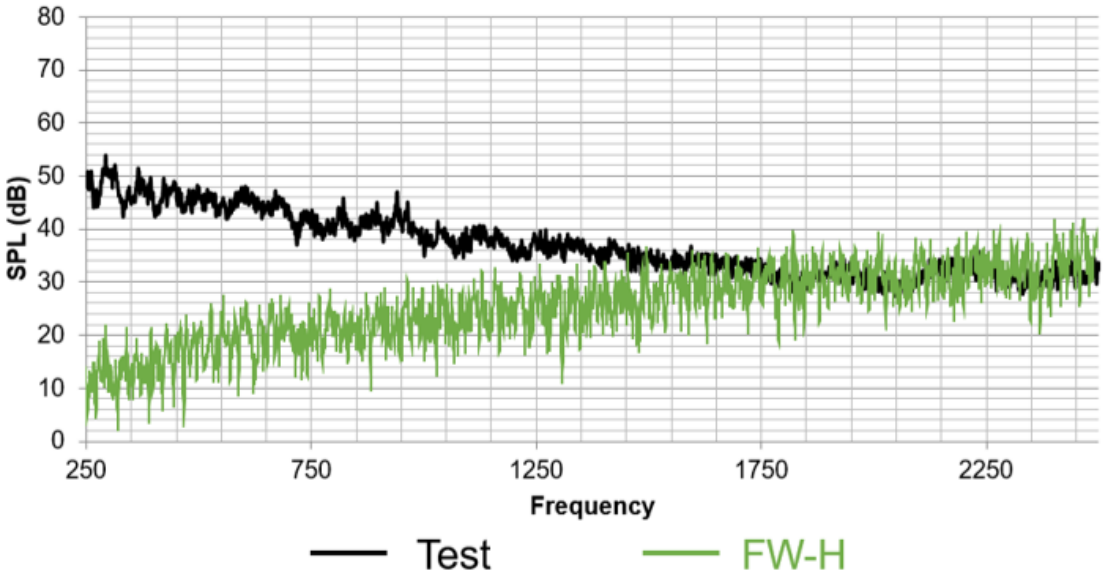

Figure 10: Sound pressure level comparison at far-field

CONCLUSION

As seen from Figure 10, low frequencies are not predicted well enough. The coherence of test and predicted values is much better at frequencies higher than 1.5 kHz.

Possible reason for the non-alignment may be due to FW-H surface choice. The best case scenario is to use a FW-H surface that contains all the turbulence. However, for a non-reduced car model, this selection is impractical.

The second possible reason is tire cavity that causes very strong pressure in the flow but not included inside the FW-H surface. Since tire cavity is not in the control surface, its acoustic effect is not observed in the acoustic calculation.

The Figure 11 shows the dominance of tire cavity in the far-field sound levels. Since only mirror and A-pillar wake regions are included in the FW-H surface, acoustic calculations are only obtained from the acoustic sources around these surfaces. As seen from Figure 11, mirror wake gets stronger after some frequency between 1kHz and 2kHz, but tire cavity is much more strong compared to mirror wake in terms of far-field noise.

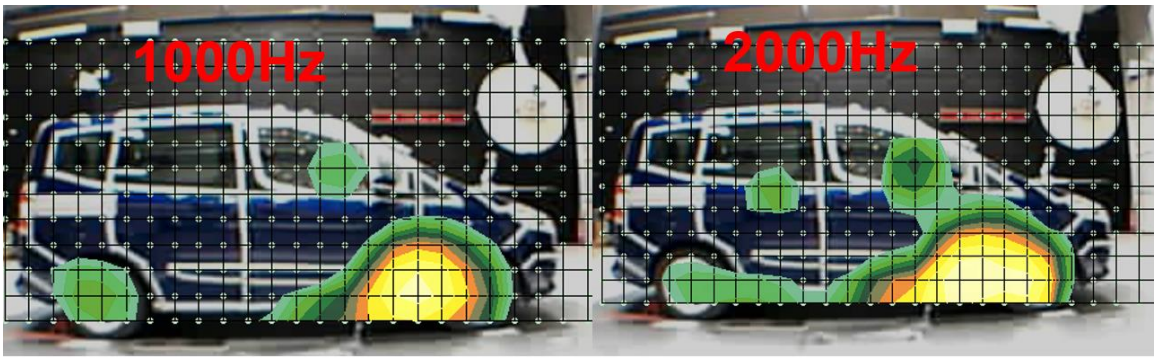

Figure 11: Aeroacoustic test results – microphone array

It is also observable from the literature that, some studies disregard cavity noise by eliminating underflow of the car; i.e. Figure 12 from [Neuhierl, Schroeck et al., 2014] is an example.

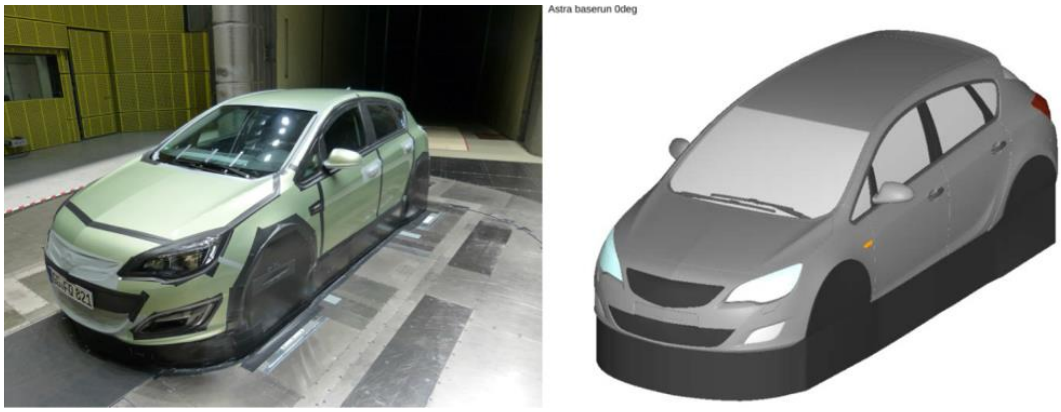

Figure 12: A study that disregards wheel cavities and underflow

The underflow and wheel cavities may be the reason of non-coherent far-field noise differences. It may also be a simplification to focus only on the main wind noise sources that driver and passengers feel the most.

Also, FW-H integration code related miscalculations are another possibilities of non-aligned SPL differences.

For these reasons, cavity noise inspection, FW-H code verification and FW-H size-location optimization tasks are next steps of this study.

References

Bergamini, P., M. Casella and D. Vitali (1997). Computational prediction of vehicle aerodynamic noise by integration of a CFD technique with Lighthill's acoustic analogy, SAE Technical Paper.
Blanchet, D., A. Golota, N. Zerbib and L. Mebarek (2014). Wind Noise Source Characterization and How It Can Be Used To Predict Vehicle Interior Noise, SAE Technical Paper.
Blanchet, D. G., Anton (2014). Wind Noise Benchmark BMT4. Summary of presentation at KSNVE 2014.
Farassat, F. and J. H. Casper (2006). "Towards an airframe noise prediction methodology: Survey of current approaches." AIAA Paper 210: 2006.
Fink, M. R. (1977). Airframe noise prediction method, DTIC Document.
Fuchs, A., E. Nijman and H.-H. Priebsch (2015). Automotive NVH Technology, Springer.
Hartmann, M., J. Ocker, T. Lemke, A. Mutzke, V. Schwarz, H. Tokuno, R. Toppinga, P. Unterlechner and G. Wickern (2012). Wind Noise caused by the A-pillar and the Side Mirror flow of a Generic Vehicle Model. 18th AIAA/CEAS Aeroacoustic Conference, AIAA paper.
Hucho, W.-H. (2013). Aerodynamics of road vehicles: from fluid mechanics to vehicle engineering, Elsevier.
Khan, I. (2014). Industrial application of CFD to predict high frequency noise from automotive acoustic devices, University of Hull.
Kotapati, R., A. Keating, S. Kandasamy, B. Duncan, R. Shock and H. Chen (2009). The lattice-boltzmann-vles method for automotive fluid dynamics simulation, a review, SAE Technical Paper.
Lockard, D. P. (2000). "An efficient, two-dimensional implementation of the Ffowcs Williams and Hawkings equation." Journal of Sound and Vibration 229(4): 897-911.
Lockard, D. P. and J. H. Casper (2005). Permeable surface corrections for Ffowcs Williams and Hawkings integrals. Proceedings of the 11th AIAA/CEAS Aeroacoustics Conference, numéro AIAA-2005-2995.
Lyrintzis, A. S. (2003). "Surface integral methods in computational aeroacoustics—From the (CFD) near-field to the (Acoustic) far-field." International journal of aeroacoustics 2(2): 95-128.
Neuhierl, B., D. Schroeck, S. Senthooran and P. Moron (2014). A Computational Aeroacoustic Study of Windshield Wiper Influence on Passenger Vehicle Greenhouse Windnoise, SAE Technical Paper.
Shorter, P., D. Blanchet and V. Cotoni (2012). Modeling interior noise due to fluctuating surface pressures from exterior flows, SAE Technical Paper.
Singer, B., D. Lockard and G. Lilley (2003). "Hybrid acoustic predictions." Computers & Mathematics with Applications 46(4): 647-669.
Sovani, S. D. and K.-H. Chen (2005). Aeroacoustics of an Automotive A-Pillar Raingutter: A Numerical Study with the Ffowcs-Williams Hawkings Method, SAE Technical Paper.
Uosukainen, S. (2011). Foundations of acoustic analogies, VTT.
Yalçın, Ö. (2015). Development Of A High-Order Navier-Stokes Solver For Aeroacoustic Predictions Of Wind Turbine Blade Sections, Middle East Technical University.
Yamamoto, K. J., M. J. Donelson, S. C. Huang and M. C. Joshi (1995). "Airframe noise prediction evaluation."
Yao, H., L. Davidson, L.-E. Eriksson, O. Grundestam, S.-H. Peng and P. Eliasson (2012). Surface Integral Analogy Approaches to Computing Noise Generated by a 3D High-Lift Wing Configuration. 50th AIAA Aerospace Sciences Meeting including the New Horizons Forum and Aerospace Exposition.
Zhengqi, G., W. Yiping and L. Weiping (2009). "Evaluation of Aerodynamic Noise Generated in a Miniature Car Using Numerical Simulation." SAE International Journal of Passenger Cars-Mechanical Systems 2(2009-01-0478): 693-702.